0

Flight dynamics model for preliminary design of PrandtlPlane wing configuration with sizing of the control surfaces [*]

F. Oliviero[a], D. Zanetti[a], V. Cipolla[a]

[a]Università di Pisa, Dipartimento di Ingegneria Civile e Industriale

Abstract

This paper deals with the evaluation of the flight dynamics response of aircraft with a PrandtlPlane configuration by means of simple models to be used during the preliminary design. The study is completed by method that allows an initial sizing of the elevator and the aileron in such the way adequate requirements can be achieved: this analysis becomes important when the control surfaces can be located in both the front and the rear wing. The flight dynamics model is carried out considering the aircraft rigid, the steady aerodynamics, and separating the longitudinal and the lateral-directional motions. In this way classic equations are considered; for both the phugoid and the short period, equations are extended taking also the Zq derivative into account because of the non-conventional wing configuration. The force derivatives are extrapolated through a VLM solver whose the reliability of the results has been proven. The sizing methods have been applied to a test case derived from the project IDINTOS; as general results, the study remarks the possibility to obtain proper longitudinal dynamic response with a reduced longitudinal Stability Margin because of the very high values of the aerodynamic damping Mq.

1. Introduction

The evaluation of the flight dynamics characteristics is not usually faced during the preliminary stage of aircraft design and, at the same time, also the control surfaces are sized in accordance to semi-empiric or statistic data. When a non conventional wing configuration is analyzed, the reliability of such these design strategies is no longer valid and a time-saving but reliable procedure to estimate the flying qualities become essential in the early stages of the aircraft design. Similar procedures, can also be used to evaluate the effects of the control surfaces on the motion of the aircraft.

In the present study, the PrandtlPlane wing configuration is considered. The PrandtlPlane architecture is based on the *Best Wing System* theory described by Prandtl [1] according to whom, the minimum induced drag occurs for a particular wing geometry, keeping both the total lift and the wingspan constant. It consists of two horizontal wings connected each other by two vertical bulkheads at the wing tips and a proper lift distribution is determined to achieve the minimum induced drag condition. Due to the Munk's stagger theorem, the two horizontal wings can be swept and moved along the asymptotic flow, without affecting the efficiency of the system so that they can be ar-

ranged in order to meet the flight mechanics requirements (namely, trim and longitudinal stability). As shown in Figure 1, the upper wing is moved to the aft of the fuselage and the front wing has a positive swept.
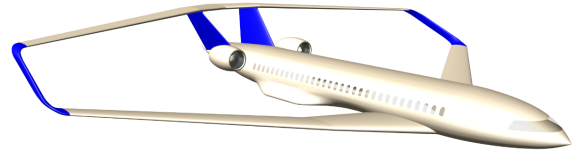

Figure 1. Artistic view of a transport PrandtlPlane aircraft

Moreover, the non-uniqueness of the solution provided by Prandtl, has been demonstrated in recent works [2] and the minimum condition can be obtained by an infinite number of solutions that differ from the reference optimal circulation only by adding an arbitrary constant; as a practical consequence of this property, the total lift can be distributed over the two horizontal wings in an arbitrary manner in order to satisfy also different design constraints (e.g. trim and stability of flight at low speed condition).

If compared with the respective wing-tail configuration (same lift and wingspan), the benefit of the PrandtlPlane configuration results in a total drag re-

duction of about 10-15% in cruise condition, depending on the non dimensional vertical gap h/b.

Apart from the aerodynamic advantage, other potential benefits can be noticed: concerning the flight mechanics aspects, the longitudinal motion appears intrinsically stable thanks to the presence of the rear wing; moreover, the elevators can be located on both the wings in such a way that, moving in opposite of phase, they produce a pure pitching moment without any changes in the total lift. Similarly, two couples of aileron can be located on the tips of both the wings, increasing the produced rolling moment per unit of length. In this context, a proper sizing procedure is requested to evaluate their effectiveness in accordance with the requirements.

At the same time, this wing geometry can result in a different flight dynamics in both the longitudinal and the lateral-directional motion so that the flying qualities have to be determined at the early preliminary design stages.

2. Dynamic Model

The flight dynamics analysis involves several aspects: aerodynamic forces have to be evaluated together with inertial properties, propulsion characteristics and control forces. All the aspects are difficult to be determined in the preliminary stages so that proper assumptions are required.

The proposed model is needed to determine the flight dynamics natural modes of the aircraft in order to evaluate if proper damping and frequencies occur.

It is based on the resolution of the linearized equilibrium equations where the aircraft is reduced to a rigid body flying in a steady straight trajectory. The approach here reported is the same described in reference [3]. Because of the symmetry of both the aerodynamic forces and the inertia properties, the longitudinal motion can be separated form the lateral-directional one so that two independent models are adopted.

2.1. Longitudinal dynamic

The longitudinal motion of the aircraft can be described by means of four state variables related to the perturbations of the equilibrium condition: two velocities u, w, the pitch angle θ and the pitch angular speed q. Considering an initial condition of straight flight (the trajectory angle θ_0 is null), the equations system 1 describes the equilibrium of the aircraft in a stability coordinates system:

$$\begin{cases} \dot{u} = X_u u + W_w w + g\theta + \Delta t \\ \dot{w} = \frac{Z_w}{1-Z_{\dot{w}}} u + \frac{Z_w}{1-Z_{\dot{w}}} w + \frac{Z_q+U_0}{1-Z_{\dot{w}}} q + \frac{Z_{\delta e}}{1-Z_{\dot{w}}} \delta e \\ \dot{\theta} = q \\ \dot{q} = \left(M_u \frac{M_{\dot{w}} Z_w}{1-Z_{\dot{w}}} \right) u + \left(M_w \frac{M_{\dot{w}} Z_w}{1-Z_{\dot{w}}} \right) w + \\ \quad + \left[M_q + \frac{M_{\dot{w}}(Z_q+U_0)}{1-Z_{\dot{w}}} \right] q + \left[M_{\delta e} + \frac{M_{\dot{w}} Z_{\delta e}}{1-Z_{\dot{w}}} \right] \delta e \end{cases} \tag{1}$$

The uppercase coefficients represent the dimensional aerodynamic derivatives respect to the quantities in the subscript. Their value is calculated from the aerodynamic non-dimensional coefficients as reported in the next paragraphs. The control is introduced in terms of elevators deflection δ_e and thrust level Δ_T. The state variables array $X_{long} = \begin{bmatrix} u & v & \theta & q \end{bmatrix}^T$ and the control array $u_{long} = \begin{bmatrix} \Delta_T & \delta_e \end{bmatrix}^T$ are introduced and, thus, the Equation 1 can be expressed in the following matrix form:

$$\dot{X}_{long} = \begin{bmatrix} A \end{bmatrix} X_{long} + \begin{bmatrix} B \end{bmatrix} u_{long} \tag{2}$$

where the coefficients, are grouped in the state matrix A and the control matrix B, respectively. Since the aim of the present model is the determination of the natural modes, the control effects can be neglected and the model is reduced to a well known eigenvalue problem:

$$|A - \lambda I| = 0 \tag{3}$$

where A is the following matrix:

$$A =$$

$$\begin{vmatrix} X_u & X_w & -g & 0 \\ \frac{Z_u}{1-Z_{\dot{w}}} & \frac{Z_w}{1-Z_{\dot{w}}} & 0 & \frac{Z_q+U_0}{1-Z_{\dot{w}}} \\ 0 & 0 & 1 & 0 \\ (M_u \frac{M_{\dot{w}} Z_w}{1-Z_{\dot{w}}}) & M_w \frac{M_{\dot{w}} Z_w}{1-Z_{\dot{w}}} & 0 & [M_q + \frac{M_{\dot{w}}(Z_q+U_0)}{1-Z_{\dot{w}}}] \end{vmatrix}$$

$$\tag{4}$$

The solutions of the characteristic Equation 3 consists of two couples of complex conjugate roots that are related to conventional phugoid and short-period modes respectively on the basis of their natural frequencies. Since the two modes involves different variables and their frequencies are far each other, they can be analyzed separately so that two explicit models are reported.

2.1.1. Short period mode

The short period mode is distinguished from variations in both vertical speed w and angular speed q whereas the variation in u can be neglected. Thus,

the system (3) can be reduced to a second order problem and it is simplified as follows:

$$\begin{vmatrix} \frac{Z_u}{1-Z_{\dot{w}}} - \lambda & \frac{Z_q+U_0}{1-Z_{\dot{w}}} \\ \left(M_w \frac{M_{\dot{w}}Z_w}{1-Z_{\dot{w}}}\right) & \left[M_q + \frac{M_{\dot{w}}(Z_q+U_0)}{1-Z_{\dot{w}}}\right]-\lambda \end{vmatrix} = 0 \quad (5)$$

Both the natural frequency ω_{sp} and the damping ζ_{sp} can be explicitly extrapolated from (5), considering that $Z_{\dot{w}} << 1$. On the contrary, the effects related to the derivative Z_q that are usually neglected for conventional wing-tail configuration, are taken into account in this case.

$$\omega_{sp} = \sqrt{\left[M_q Z_w - M_w Z_q + M_\alpha\right]}$$

$$\zeta_{sp} = -\frac{1}{2\omega_{sp}}\left[M_q + Z_w + M_{\dot{w}}Z_q + M_{\dot{\alpha}}\right] \quad (6)$$

2.1.2. Long period mode

During the phugoid motion, the variations of vertical speed w are negligible if compared with variation in longitudinal speed u and the pitch angle θ. In this case, the pitch equilibrium is verified and the third expression in Equation 1 is no longer considered so that the correspondent eigenvalue problem can be reduced as follows:

$$\begin{vmatrix} X_u - \lambda & -g \\ \frac{Z_u}{Z_q+U_0} & 0 \end{vmatrix} = 0 \quad (7)$$

Similarly to the short period case, both the natural frequency and damping can be explicitly determined for the phugoid motion remarking that the force damping Z_q is taken into account due to the non conventional wing configuration.

$$\omega_{ph} = \sqrt{-g\frac{Z_u}{Z_q+U_0}}$$

$$\zeta_{ph} = -\frac{X_u}{2}\sqrt{-g\frac{Z_q+U_0}{gZ_u}} \quad (8)$$

2.2. Lateral-directional dynamics

Referring to the stability coordinate system and assuming an initial condition of straight flight (the bank angle $\Phi_0 = 0$), the aircraft motion can be described by the following system:

$$\begin{cases} \dot{v} = Y_v v + Y_p p + (Y_r + U_0)r + g\phi + Y_{\delta r}\delta_r \\ \dot{p} = L'_v v + L'_p p + L'_r r + L'_{\delta a}\delta_a + L'_{\delta r}\delta_r \\ \dot{r} = N'_v v + N'_p p + N'_r r + N'_{\delta a}\delta_a + N'_{\delta r}\delta_r \\ \dot{\phi} = p \end{cases} \quad (9)$$

In this case the variable states array X_{ld} is composed by the lateral speed $v = U_0\beta$, the rotational

speed along the x-axis and z-xis (p and r respectively) and the bank angle ϕ. The control variables are represented by the deflections of the ailerons and the rudder. It can be remarked that the *primed forces derivatives* appearing in Equation 9, are introduced in order to uncouple the rotational equilibrium along the x-axis and z-axis (second and third expressions of Equation 9) because of the presence of the inertial term I_{xz}. The primed derivatives can be expressed in terms of usual forces derivatives by using the following formula:

$$\left\{ \begin{array}{c} L'_i \\ N'_i \end{array} \right\} = \frac{1}{\Delta}\left[\begin{array}{cc} 1 & I_{xz}/I_x \\ I_{xz}/I_z & 1 \end{array} \right]\left\{ \begin{array}{c} L_i \\ N_i \end{array} \right\} \quad (10)$$

The natural modes are determined by solving the characteristics equation of the homogeneous system as reported in Equation 11:

$$\left|A_{ld} - \lambda I\right| = \begin{vmatrix} Y_v - \lambda & Y_p & (Y_r + U_0) & g \\ L'_v & L'_p - \lambda & L'_r & 0 \\ N'_v & N'_p & N'_r - \lambda & 0 \\ 0 & 1 & 0 & -\lambda \end{vmatrix} = 0$$

$$(11)$$

The characteristics Equation 11 consists of two real roots and a couple of conjugate complex roots; the real roots (T_r and T_s) are associated to roll and spiral mode respectively while the two complex roots are related to the dutch roll mode with frequency ω_{dr} and damping ζ_{dr}. The natural modes are computed directly by solving the eigenvalue problem of Equation 11 even though explicit relations can be assumed under the hypothesis of neglecting some of the force derivatives. These last assumptions, valid for conventional wing configuration, cannot be verified in general, for the PrandtlPlane. Thus, the approximated solutions reported in (12) will be compared with the roots of Equation 11.

$$T_r \cong L'_p$$

$$T_s \cong \frac{g}{U_0}\frac{L'_v N'_r - N'_v L'_r}{L'_v N'_p - N'_v L'_p}$$

$$\omega_{dr} \cong \sqrt{Y_v N'_r + U_0 N'v}$$

$$\zeta_{dr} \cong -\frac{Y_v + N'r}{2\omega_{sp}} \quad (12)$$

3. Flying and Handling qualities

The dynamic characteristics, together with the stability and maneuverability aspects, contribute to define the so called *flying qualities* of the aircraft. Thus, the *flying qualities* are related to the response of the aircraft during each mission segment, being dominated by the physical flight parameters (e.g. Stability Margin, dynamics frequencies and damping).

The effectiveness of these responses cannot be evaluated easily since they are strictly related to the way of piloting and to the human perception. For this reason, the concept of the *handling qualities* is introduced, referring to the ease and precision which a pilot can accomplish a particular mission with.
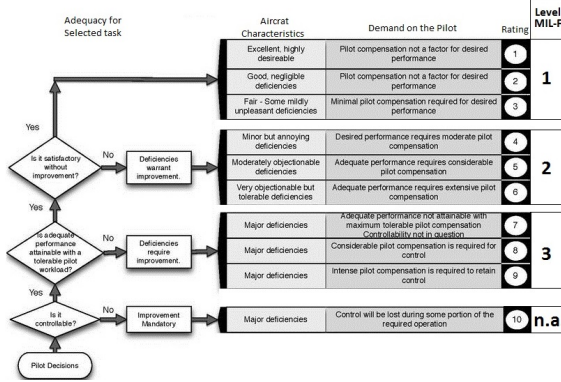

Figure 2. Cooper-Harper scale

The *Cooper-Harper* [4] scale is a common criterion used by pilots and engineers to evaluate the handling qualities by assigning a value from 1 (best) to 10 (worst) to the response of the aircraft in a particular mission task; the rating scale reported in Figure 2 remains difficult to be interpreted since it involves the pilot-in-the-loop and other effects due to the control systems (e.g. differences between fly-by wire or mechanical controls).

In the present study, the handling qualities are compared to the flying qualities by using the *MIL-F-8785C* procedure [5], that provides an equivalent classification to the Harper-Cooper scale on the basis of the dynamic and static characteristic of the aircraft: the correspondent rating is reported in the same Figure 2. Three different *level of compliance*, from 1 (the best) to 3 (just satisfactory) are specified for four different classes of aircraft (denoted with Roman number I to IV) and for three Flight Phases (named A, B and C). Both the aircraft and the mission classifications are defined in the following Table.

The procedure is usually applied to military aircraft and thus, in case of civil application, both the specifications relative to the aircraft class *IV* and the flight phases *A* are no longer valid. In particular, some constraints for both the longitudinal and the lateral-directional natural modes can be extrapolated from [5] as reported in the following sub-paragraphs.

Table 1
Classification of aircraft classes and flight phases

MIL-F-8785C	Aircraft classes
I	Small, light airplanes
II	Medium weight, low-to-medium maneuverability airplanes
III	Large, heavy, low-to-medium maneuverability airplanes
IV	High-maneuverability airplanes

MIL-F-8785C	Flight phase categories
A	Flight Phases that require rapid maneuvering
B	Non terminal Flight Phases (Climb, Cruise, Loiter)
C	Terminal Flight Phases

3.1. Requirements on the longitudinal flying qualities

The reference [5] provides limits on the natural modes of the aircraft as far as on the control forces perceived form the pilot during maneuvers. In this study, only the requirements directly related to the dynamic modes are considered. Limits on both the phugoid and short period damping are provided, independently from the class of the considered aircraft as reported in Table 2. The limits on the phugoid damping are also valid for any flight category while differences are reported in the case of the short period motion.

Table 2
Limits on the longitudinal damping

Level	Phugoid	Short Period Cat.B	Short Period Cat.C
1	$\zeta_{ph} > 0.004$	$\zeta_{sp} \in (0.3, 2.0)$	$\zeta_{sp} \in (0.35, 1.3)$
2	$\zeta_{ph} > 0$	$\zeta_{sp} \in (0.3, 2.0)$	$\zeta_{sp} \in (0.25, 2.0)$
3	$T > 55sec.$	$\zeta_{sp} > 0.15$	$\zeta_{sp} > 0.15$

The short period natural frequency, can be limited by introducing the *Control Anticipation Parameter* defined as the ratio between the initial angular speed at the beginning of a certain maneuver, and the normal acceleration when steady state condition are reached.

$$CAP \equiv \frac{q}{\Delta n} \approx \frac{\omega_{sp}^2}{\frac{U_0}{g}\frac{1}{T_{\Theta 2}}} \approx \frac{\omega_{sp}^2}{n/\alpha} \qquad (13)$$

where the term $1/T_{\Theta 2}$ represents the zero of the high
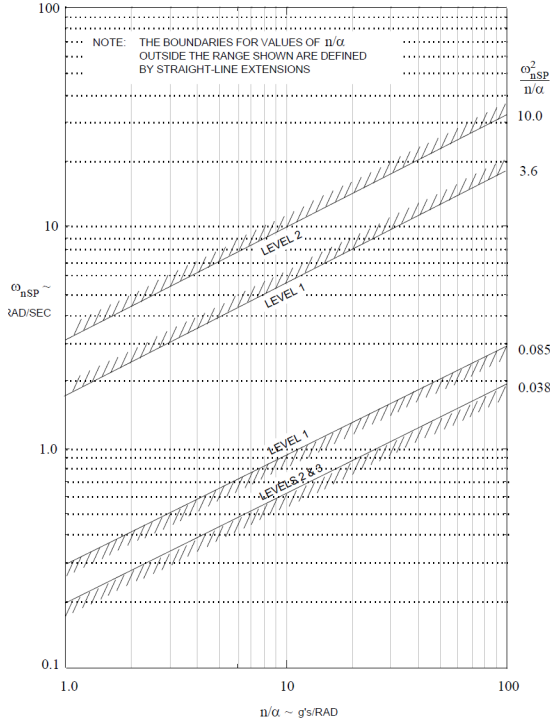
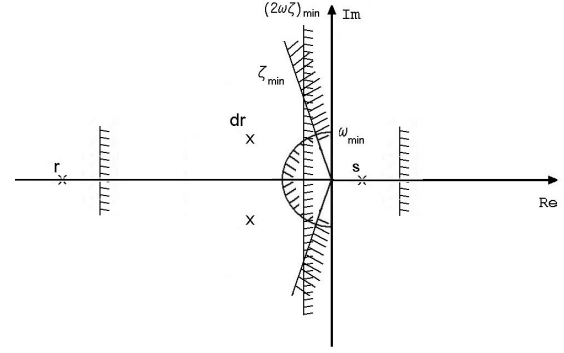Figure 3. Limits on the CAP for flight phases B

Figure 4. Limits of the lateral directional poles

$$\frac{1}{T_s} = \frac{ln(2)}{\Delta_{T2}} \quad (15)$$

3.3. Additional requirements on the control surfaces

No direct specifications on the dimensions and effectiveness of the mobile surfaces are indicated in [5].Thus,the elevators are sized in such a way that a prescribed maximum vertical load factor is reached. By using the short period model, the maximum load factor can be determined depending on a given deflection of the elevator:

$$n_{zmax} = 1 + \frac{U_0}{g} \frac{Z_{\delta_e}}{(U_0 + Zq)} \cdot \frac{\left(1 + \frac{M_{\delta_e} Z_\alpha}{Z_{\delta_e} M_\alpha}\right)}{1 - \frac{Z_\alpha Mq}{(U_0 + Zq)M_\alpha}} \cdot \delta_e \quad (16)$$

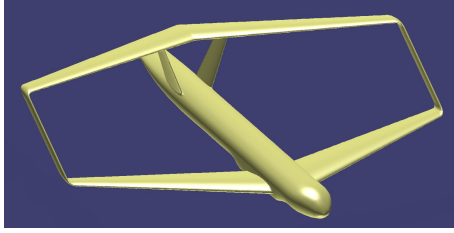The maximum deflection of the elevator is evaluated on the basis on the trim condition.

The rolling angular speed at steady condition can be evaluated for a given aileron deflection as follows:

$$P_\infty = T_r L'_{\delta_a} \delta_a$$

In the present study, it is supposed that both the maximum load factor and the rolling angular speed are imposed, so that a correspondent deflection of both the mobile surfaces can be determined.

4. Sizing procedure

An automated procedure is set up in order to determine both the flying qualities and the effects of the mobile surfaces (elevators and ailerons) for a given wing geometry. Initial data are directly extrapolated from an in-house developed parametric geometric generator [6] (an example of the generated geometry is reported in Figure 5) together with the definition of reference flight parameters.

frequency pitch attitude. In the present work it has been determined by solving the system 1 respect to the variable θ/δ_e, by applying the Cramer method and obtaining the following expression:

$$\frac{1}{T_{\theta 2}} = -Z_w(1 - \frac{Z_{\delta e}}{M_{\delta e}} \frac{M_w}{Z_w})/(1 + \frac{Z_{\delta e}}{M_{\delta e}} M_{\dot{w}}) \quad (14)$$

Some limits are imposed to the maximum and minimum values of CAP, as reported in Figure 3, so that correspondent limitations on the natural frequency can be determined by means of the Equation 13.

3.2. Requirements on the lateral directional flying qualities

Direct limits are imposed to the dutch roll frequency and damping: these limits depend on both the flight phase category and the aircraft class. Similarly, the maximum roll mode time constant is given depending on both the two parameters.

The limits are (qualitatively) reported in Figure 4 in the framework of the imaginary plane of the poles, while the values can be directly taken from [5].

On the other hand, a divergent spiral motion with negative value of the damping is admitted: in this case the minimum time Δ_{T2} to double the amplitude is imposed, depending only on the flight phase category. It is remarked that it can be related to the spiral pole by using the relation:

Figure 5. Geometric generation with *ASD* software

Two different procedures are available for the longitudinal and the lateral-directional analysis respectively; as shown in Figures 6 and 7, an iterative procedure has been set up in both the cases to size the mobile surfaces: their lengths are progressively increased until adequate levels of vertical load factor and rolling angular speeds are achieved. At the same time, the procedure gives information on the levels of the flying qualities; if they are not satisfactory, the wing geometry needs to be redesigned properly.
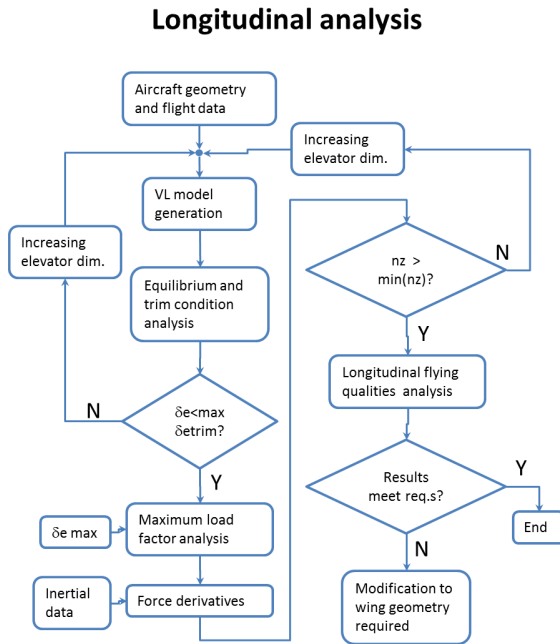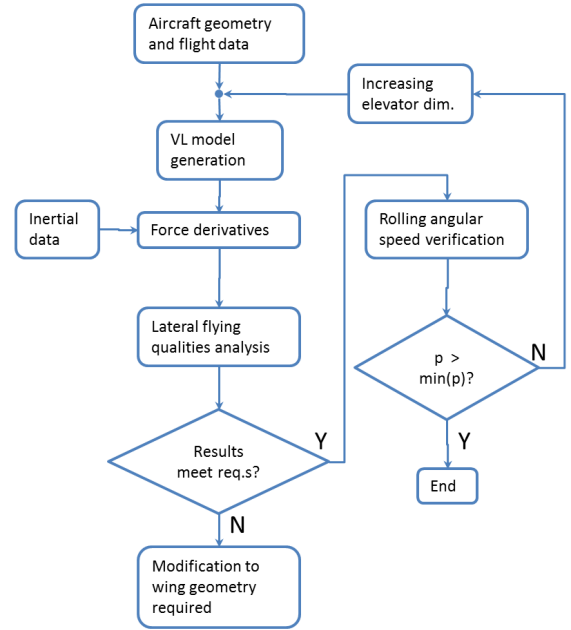
Lat.-dir. analysis

Figure 7. Calculation procedure for lateral-directional dynamics

Vortex Lattice Method [7] is used; in previous works (e.g. [8]), the code has been calibrated for the analysis of PrandtlPlane wing configurations and an example of the used VLM grid is reported in Figure 8.
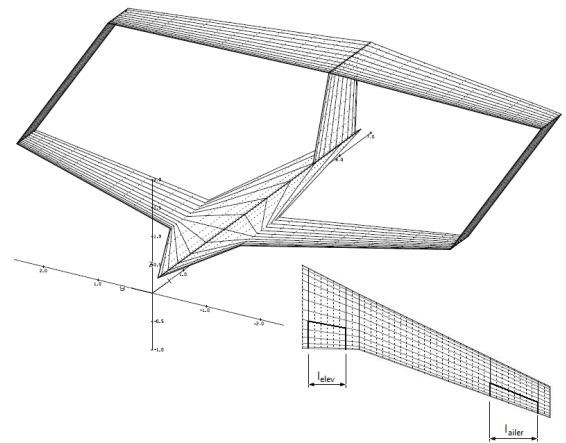
Longitudinal analysis

Figure 6. Calculation procedure for longitudinal dynamics

Figure 8. VLM model of a PrandtlPlane

A preliminary aerodynamic analysis is needed to determine the aerodynamic coefficients and consequently the force derivatives used in the models described in the paragraph 2. In this case, a software based on a

The fuselage is modeled as a part of the front wing

with a proper dihedral angle in such a way that the lateral size is replicated. The code allows to include mobile surfaces by indicating the grid cells of the wings that are interested by the deflection. In the case of the PrandtlPlane wing configuration, elevators and ailerons are located on both the front and the aft wings.

The aerodynamic coefficients determined by the VLM analysis have been validated by proper comparison with Wind Tunnel tests conducted for a particular wing geometry ([9]) relevant to the *IDINTOS* project ([10]): both the elevators and the ailerons are modeled in the wind tunnel test model so that also the derivatives respect with their deflections can be extrapolated. The comparisons between VLM results and wind tunnel measurements are reported in the graphs of Figures 9 and 10; it is noticed that, although the VLM code provides also the derivatives with respect the angular velocities, they are not evaluated in the Wind Tunnel tests.
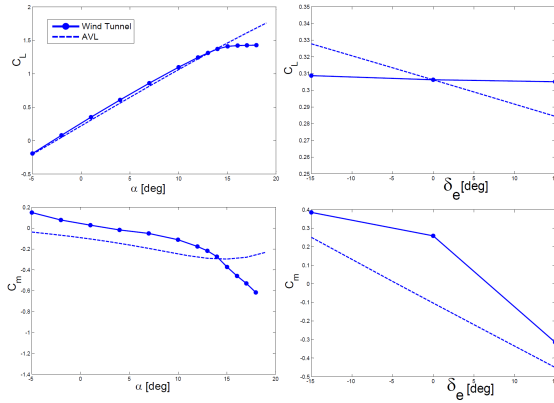

Figure 9. Longitudinal aerodynamic coefficients comparison

Some differences can be appreciated in terms of absolute values of the aerodynamic coefficients, mainly due to the difficult computation of the friction drag. On the other hand, the results of the VLM analysis are satisfactory in terms of derivatives if a linear aerodynamic field is valid (small Angle of Attack, and small deflections): in this case, the largest differences are within the 10 % in the case of the derivatives with respect the aileron deflection. Thus, the results coming form the VLM analysis are assumed to be valid for the presents study also including those concerning the angular velocities. Since the aerodynamics coefficient are calculated, the force derivatives are determined by considering the flight condition in terms of speed U_0 and altitude following the relations reported in [3]. In-
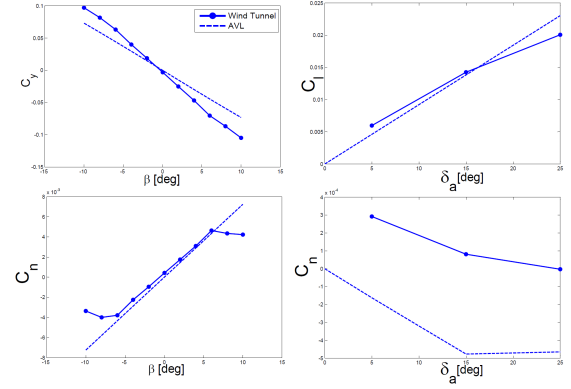

Figure 10. Lateral-Directional aerodynamic coefficients comparison

ertial data, have to be also included and, assuming that the inertia matrix is known, it is rotated by the AoA determined in trim condition, in order to report its components in the stability coordinate system.

5. Application to IDINTOS project

As test case, the *IDINTOS* aircraft has been considered because of the reliability of the aerodynamic data from the VLM analysis.

Co-founded by the Regional Government of Tuscany (Italy) between 2011 and 2013, the IDINTOS project has faced the design of a ultralight amphibious PrandtlPlane and the manufacturing of a flying prototype. A consortium of universities and private companies participated to the project, under the leadership of University of Pisa ([10], [9]).

The amphibian, shown in Figure 11, is a side-by-side two-seater and it is provided with a floating fuselage, retractable landing gears, an engine which drives two ducted propellers and two wingtip auxiliary floats. Such aircraft has been designed in order to fulfill the requirements defined by the Italian regulation on sport aircraft. As shown in in Figure 11, elevators (in red) and ailerons (in green) are placed on both rear and front wings.

The flying qualities are thus analyzed for two flight conditions: the first one deals with a low speed condition $U_0 = 20$ m/s and $h = 0$ and the second one is related to cruise condition $U_0 = 50$ m/s, $h = 1000$ m. Results are reported in Table 3, assuming a Stability Margin $SM = 16\%$ and a reference mass $W = 525$ kg:

If compared with an equivalent general aviation aircraft with classic wing tail configuration [11], the force derivatives present slight differences: in particular it is remarked that the aerodynamic damping Cmq results about three time higher than in the wing tail configuration as far as the pitch stiffness $C_{m\alpha}$. These values
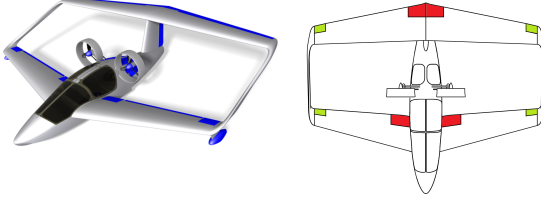
Figure 11. IDINTOS aircraft

gible if compared with those ones of traditional configurations; this response have potential benefits on the safety of flight, specially at low altitudes, because the total produced lift doesn't vary during pull-up maneuvers. At the same time, the pitch moment results adequate also if values in low speed condition results very close to the lower limit. This problem can be solved by varying the SM of the aircraft; as an example, we consider the longitudinal poles reported in Figure 12 when the SM varies in a range [+50% -10%].

Table 3
Results for IDINTOS aircraft

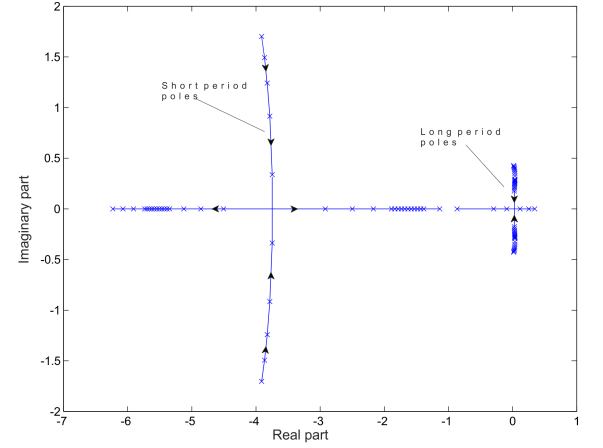| **Longitudinal**	$V = 20$	$V = 40$
Force derivatives		
Zw	-1.612	-3.3972
Zq	-1.857	-4.4752
$Z\delta_e$	-0.5638	-1.5249
Mw	-0.134	-0.2490
Mq	-3.600	-6.8649
$M\delta_e$	4.826	18.5692
$M\alpha$	-2.672	-9.9611
Flying qualities		
ω_{ph}	0.69	0.28
ζ_{ph}	0.1615	0.034
ω_{sp}	2.87	4.9
ζ_{sp}	1.134	1.01
n_{zmax}	2.4	7.1
CAP	2.1	2.01
Lat-Dir	$V = 20$	$V = 40$
Force derivatives		
Yv	-0.161	-0.2236
$L'\beta$	-3.88	-5.5183
$N'\beta$	0.464	1.7784
$L'p$	-1.661	-3.823
$N'p$	-0.047	-0.4277
$L'r$	1.241	0.4695
$N'r$	-0.4852	-0.20194
$L'\delta_a$	2.453	4.1429
$N'\delta_a$	-0.031	-0.3280
Flying qualities		
ω_{dr}	0.82	1.22
ζ_{dr}	0.143	0.155
$\tau_r[sec]$	0.47	0.26
$\Delta_{T2}[sec]$	28	> 100
$p_\infty[deg/sec]$	11.4	16.2

Figure 12. roots locus of the longitudinal poles

Decreasing the SM, both the short period and the phugoid poles move towards the real axis; consequently, one of the phugoid pole tends to the positive part of the plane becoming critic for a value of the $SM = 0$. On the other hand, the two modes coalesce so that the assumption to divide the analyses becomes no longer valid. In this context, the short period damping becomes critic for a value of the $SM = 2\%$ as shown in Figure 13 together with the variations of the maximum load factor.
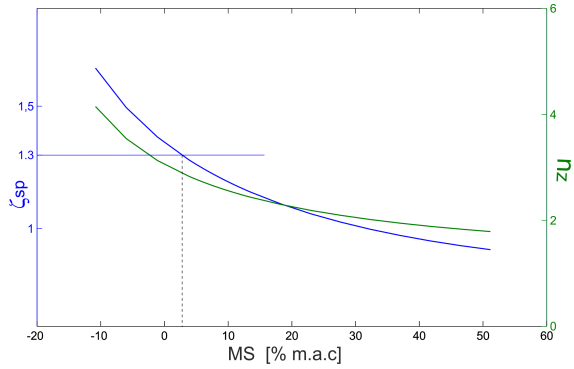
As expected, the maximum load factor n_{zmax} increases as the SM decreases and the longitudinal maneuverability of the aircraft is then enhanced. At the critic condition determined by the value of the short period pole $\zeta_{sp} = 1.3$, the maximum value of the load factor is $n_z = 3.1$.

Most of the other flying qualities are within the *level 1* defined on specifications [5], except the phugoid damping (level 2) during the cruise condition. The force derivatives in the lateral-directional plane are notably different if compared with those of conventional wing-tail reference because of the contribution of the lateral bulkheads: nevertheless the lateral-directional flying qualities result not critic.
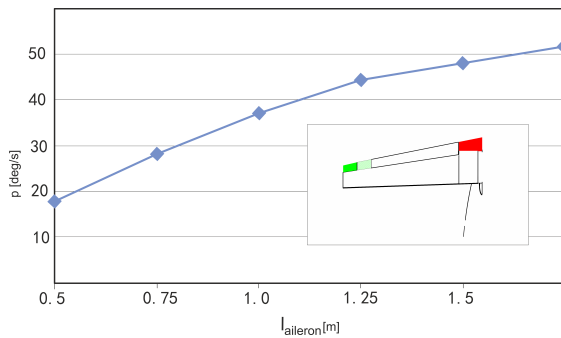
have mainly consequences on the short period mode, that is over-damped ($\zeta_{sp} > 1$) resulting in an aperiodic motion; nevertheless, this response is within the limit imposed for the *level 1* of the specifications.

The two couples of elevators, acting in opposite of phase, produce a pure pitch moment being Z_{δ_e} negli-

Figure 13. n_z and ζ_{sp} vs SM

The rolling angular speed, obtained with an initial aileron length $l_{ailer} = 0.375$ m, is not adequate in the low speed condition so that the iterative procedure reported in Figure 7 is used to size them. The sizing procedure regards only the ailerons of the rear wing due to low speed limitations on the flap system. In Figure 14 the steady rolling speed is shown at varying the length of the rear ailerons.

Figure 14. p_∞ vs l_{ailer}

The *level 3* (equal to a rolling speed $p=23$ [deg/s]) can be obtained for an aileron length $l_{ailer} = 0.67$ m; in this case the problem is solved by doubling their initial length so that a final rolling speed $p = 28$ [deg/s] is achieved.

6. Conclusion

In this paper, an automated procedure for the preliminary evaluation of the flying qualities is presented. The procedure has a general validity and it is applied to classic wing tail configuration as a validation test cases with positive results (here not reported). The procedure extrapolates the force derivatives by means of a VLM aerodynamic code, whose results has been validated for the case of PrandtlPlane configurations through the comparison with Wind Tunnel tests.

The geometry of the *IDINTOS* aircraft is taken into account to analyze the flying qualities of the PrandtlPlane configuration. Results show that the dynamic response meets the handling qualities prescribed in [5] for both the longitudinal and the lateral-directional plane.

As general results, the PrandtlPlane configuration allows to control the pitch without any variations of vertical lift, as shown in the computation of the force derivatives with respect the deflection of the elevators. This result improves the safety for those flight conditions occurring at low altitudes. At the same time, this configuration presents very high values of both the pitch damping and the pitch stiffness so that the longitudinal maneuverability can represent a critical aspect. Nevertheless the Stability Margin of the aircraft can be reduced without any degradation of the flying qualities and static stability of flight.

The effectiveness of the two couples of aileron is partially reduced by the increased inertia of the aircraft. Thus the initial ailerons are not big enough to guarantee an adequate rolling speed in steady condition. As a results of the sizing procedure, the length of the rear wing ailerons has been doubled in order to fulfill the requirements.

REFERENCES

1. Prandtl, L., "Induced drag of multiplanes," Tech. Rep. TN-182, NACA, 1924.
2. Demasi, L., Monegato, G., Rizzo, E., Cavallaro, R., and Dipace, A., "Minimum induced drag theorems for joined wings, closed systems, and generic biwings: Results," *56th AIAA/ASCE/AHS/ASC Structures, Structural Dynamics, and Materials Conference*, 2015, p. 0698.
3. Casarosa, C., *Meccanica del volo*, Plus-Pisa University Press, 2004.
4. Harper, R. P. and Cooper, G. E., "Handling qualities and pilot evaluation," *Journal of Guidance, Control, and Dynamics*, Vol. 9, No. 5, 1986, pp. 515–529.
5. Various, A., "MIL-F-8785C: Flying qualities of Piloted Airplanes," Tech. rep., USA Military Specification, 1991.
6. Cavallaro, R., *A code for surface modeling and grid generation coupled to a panel method for aerodynamic configuration design*, Master's thesis, University of Pisa, 2009.
7. Drela, M. and Youngren, H., "AVL 3.30 User Primer," Tech. rep., 2010.
8. Cipolla, V., *Utilizzo di codici a pannelli nel progetto preliminare di velivoli prandtlplane ultraleggeri; applicazione a nuove configurazioni*, Master's

      thesis, University of Pisa, 2006.

9.   Cipolla, V., Frediani, A., Gibertini, G.,
      and Oliviero, F., "A ultralight amphibious
      PrandtlPlane: wind tunnel tests," *AIDAA XXII
      Conference Proceedings*, 2013.

10.   Frediani, A., Cipolla, V., and Oliviero, F., "Design
      of a prototype of light amphibious PrandtlPlane,"
      56th AIAA/ASCE/AHS/ASC Structures, Structural Dynamics, and Materials Conference, 2015,
      p. 0700.

11.   Schmidt, L. V., *Introduction to aircraft flight dynamics*, AIAA, 1998.